



## Simulation of the regional climatic effect of irrigation over the Yellow River Basin

Liang CHEN, Zhu-Guo MA, Tian-Bao ZHAO, Zhen-Hua LI & Yan-Ping LI

**To cite this article:** Liang CHEN, Zhu-Guo MA, Tian-Bao ZHAO, Zhen-Hua LI & Yan-Ping LI (2017) Simulation of the regional climatic effect of irrigation over the Yellow River Basin, Atmospheric and Oceanic Science Letters, 10:4, 291-297, DOI: [10.1080/16742834.2017.1313681](https://doi.org/10.1080/16742834.2017.1313681)

**To link to this article:** <https://doi.org/10.1080/16742834.2017.1313681>



© 2017 The Author(s). Published by Informa UK Limited, trading as Taylor & Francis Group



Published online: 24 Apr 2017.



Submit your article to this journal



Article views: 1577



View related articles



View Crossmark data



Citing articles: 3 View citing articles

## Simulation of the regional climatic effect of irrigation over the Yellow River Basin

CHEN Liang<sup>a</sup>, MA Zhu-Guo<sup>a</sup>, ZHAO Tian-Bao<sup>a</sup>, LI Zhen-Hua<sup>b</sup> and LI Yan-Ping<sup>b</sup>

<sup>a</sup>CAS Key Laboratory of Regional Climate-Environment for Temperate East Asia, Institute of Atmospheric Physics, Chinese Academy of Sciences, Beijing, China; <sup>b</sup>Global Institute for Water Security, University of Saskatchewan, Saskatoon, Canada

### ABSTRACT

In this study, the authors developed a new irrigation scheme based on the Noah land surface model, and then coupled it with the Weather Research and Forecasting regional climate model. Two simulations (with and without irrigation) were conducted over the Yellow River basin for the period April to October 2000–2010. The results indicated that the WRF model is able to successfully capture the spatial pattern and seasonal changes in observed temperature and precipitation over the Yellow River basin. When irrigation was induced, the mean surface air temperature at 2 m ( $T_{2m}$ ) decreased by 0.1–0.4 K, and there was a correspond increase (decrease) in latent (sensible) heat flux over the irrigated areas, wherein the increase (decrease) reached more than 10 W m<sup>-2</sup> over the largest irrigated areas. The cooling effect was consistent with the changes in evapotranspiration and heat fluxes due to irrigation. The changes in lifting condensation level and planetary boundary layer height led to a greater probability of cloud formation and bore a close association with surface fluxes and soil moisture, which then impacted the spatial distribution of  $T_{2m}$  and precipitation.

### 摘要

本文基于新设计的灌溉参数化方案，并将其耦合到区域气候模式WRF之中，利用此模式对黄河流域进行为期10年的区域气候模拟，结果显示引入灌溉之后将减小模拟的土壤湿度，感热和潜热的偏差。灌溉导致地表增加额外的水分，从而导致土壤湿度和蒸发增加，地面空气冷却，感热减小和潜热增加，同时导致行星边界层也发生变化。揭示了农业灌溉在区域气候研究中的重要性和增强对人类活动在调节陆-气-云相互作用的理解。

### ARTICLE HISTORY

Received 19 December 2016

Revised 7 March 2017

Accepted 9 March 2017

### KEY WORDS

Irrigation; WRF; regional climate

### 关键词

灌溉; WRF; 区域气候

## 1. Introduction

Humans are changing the regional climate not only by replacing land cover but also through changes in land management, including agricultural irrigation (Leng et al. 2014). It is reported that, globally, irrigated agriculture consumes more than 2600 km<sup>3</sup> of water each year, which comprises 70% of all human water withdrawal (Shiklomanov 2000; Douglas et al. 2009). The huge amount of water used for irrigation has a significant impact on near-surface energy exchange and the hydrological cycle. First, irrigation reduces the surface albedo, and increases the evapotranspiration and net surface radiation (Kueppers, Snyder, and Sloan 2007). By delivering more additional water to the land surface, the soil moisture increases, and leads to increased evapotranspiration and decreased near-surface air temperature.

In recent years, most observed and simulated results have shown that the average temperature and daily maximum-temperature days in agricultural irrigation areas has decreased, along with increased precipitation (Barnston and Schickedanz 1984; Moore and Rojstaczer 2001; Adegoke et al. 2003; Adegoke, Pielke, and Carleton 2007; Pielke et al. 2007; Lobell and Bonfils 2008; Diffenbaugh 2009; Lee et al. 2009). Sacks et al. (2009) analyzed the effects of global irrigation on near-surface temperature, and found that the effects of agricultural irrigation on the global average temperature can be ignored, but a very significant cooling effect at regional scales over irrigated agricultural areas can be detected.

The Yellow River basin lies in the central and northern part of China and its drainage area is about 795,000 km<sup>2</sup>. The climate is arid or semi-arid over most regions of the Yellow River basin. The river runoff is relatively low, with

water shortages in its drainage. The annual precipitation is less than 400 mm over 1/3 of the river basin, and 400–800 mm for the rest of the river basin. The mean annual precipitation for the whole basin is 466 mm, and the average annual evaporation is 1100 mm (Yu, He, and Chen 2003). As a sensitive area in terms of global climate change, the Yellow River basin is situated in arid and semiarid regions and also plays an important role in food production. However, the utilization of water resources in the Yellow River basin is facing a considerable challenge due to drought and the increasing consumption of water. Large-scale agricultural irrigation is an important part of the utilization of water resources in the Yellow River basin. Thus, applying irrigation effectively in the Yellow River basin, and in such a way that minimizes the adverse effects in terms of regional climate change, is a scientific problem in need of answers.

Large-scale agricultural irrigation mainly acts to change surface water processes, and then affects the regional climate. Indeed, this regional climate effect of changes in soil moisture has been the topic of much research work in China. Ma, Wei, and Fu (1999) indicated that the relationship between soil moisture and precipitation is positively correlated with temperature in East China. Furthermore, according to research using a hydrological model to simulate the effects of agricultural irrigation in the Yellow River region, Tang et al. (2007) found that, due to the presence of irrigation, runoff decreased by up to 41% in the Yellow River basin at the peak of irrigation (June, July, and August), the average latent heat (LH) flux increased by  $3.3 \text{ W m}^{-2}$ , and the surface average air temperature decreased by 0.1 K.

In summary, the agricultural irrigation area of the Yellow River basin has continued to grow (Lei, Jia, and Xiao 2013), which in turn has changed the surface water balance significantly. In the present study, based on global irrigation area data (Siebert et al. 2005), we extracted model grid unit agricultural irrigation area ratio data as the driving mode. The newly developed irrigation scheme within the Noah land surface model was coupled into a high resolution regional climate model, and then the improved coupled regional climate model was used to analyze the effects of agricultural irrigation on climate change and land–atmosphere interaction over the Yellow River basin.

## 2. Model and experiment design

To assess the impacts of irrigation on temperature, precipitation, and surface fluxes over the Yellow River Basin, two simulations (hereafter referred to as CTL and IRR)

were performed using the WRF model (version 3.6.1). Each of the simulations had ten summers (2001–2010), with the initial conditions at 0000 UTC 1 April and ending at 0000 UTC 1 October. The first two months were treated as the spin-up period, and the output in the last four months of each year were analyzed in this study. The WRF model was integrated over a domain covering the entire area of the Yellow River Basin, with a central point at (37.1°N, 107.3°E). The horizontal resolution was 10 km, with 216 grid points in the east–west direction and 122 grid points in the north–south direction. There were 51 vertical atmospheric levels, with the model top at 50 hPa. The model domain is shown in Figure 1(a), including three sub-regions outlined by the boxes that are used for summarizing the statistical analysis. The sub-regions shown in Figure 1(a) represent three typical irrigation areas over the Yellow River basin, and were chosen based on land cover data indicating the areas were dominated by cropland (Figure 1(a)) and the irrigation area fractions were larger than 50% (Figure 1(c)). The time step was 60 s. The simulation was forced with 6-h 0.7° ERA-Interim reanalysis data (Dee et al. 2011). The physical parameterization schemes in the WRF model were the same as in Chen et al. (2016). To investigate the effect of irrigation on surface fluxes and land–air interactions, we implemented the irrigation algorithm of Ozdogan et al. (2010) and Qian et al. (2013) in the Noah land surface model. First, we aggregated the 500-m MODIS-based irrigated land map and area data (Ozdogan and Gutman 2008; Ozdogan et al. 2010) to irrigation fractions at 10-km resolution, consistent with the WRF domain, to represent the fraction of each grid cell that could potentially be irrigated as needed (Figure 1(b)). The land cover map indicated that the irrigation area fraction of the study domain is mainly covered by cropland (Figure 1(c)). Then, we applied irrigation to the grid cells covered by cropland when the irrigated fraction in Figure 2(a) was above zero during the growing season. The length of the growing season was calculated based on the greenness fraction (GF) (Qian et al. 2013), given by

$$GF_{\text{thresh}} = GF_{\min} + 0.4 \times (GF_{\max} - GF_{\min}), \quad (1)$$

where  $GF_{\min}$  and  $GF_{\max}$  are the annual minimum and maximum greenness fractions in grid cells, and  $GF_{\text{thresh}}$  is set as the threshold to represent the start and end of the growing season. Irrigation is triggered when the soil moisture availability in any root-zone layer drops below minimum (0.5 in this study), the soil moisture in all root layers is set to the specified target level (1.0), and irrigation only takes place between 0600 local time (LT) and 1000 LT during the growing season. Moisture availability is defined as

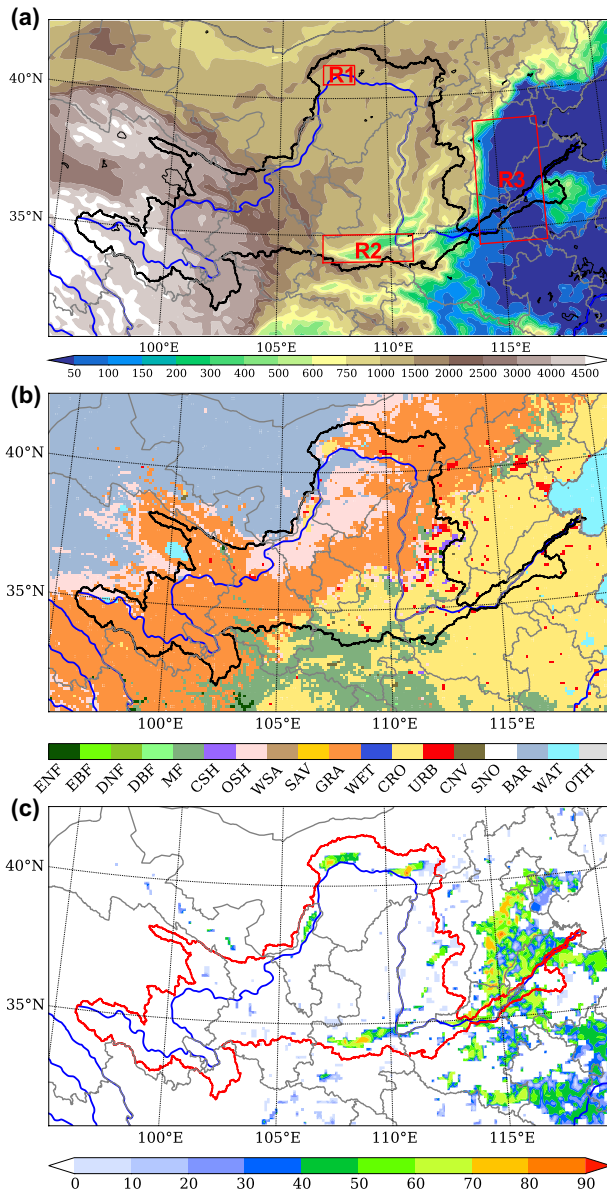


**Figure 1.** (a) The WRF model domain and topography used in this study (units: m); the horizontal resolution is 10 km. (b) MODIS land cover/land use maps of the study domain. (c) MODIS potential irrigation area fraction (%) from Ozdogan and Gutman (2008). The regions labeled R1, R2, and R3 in (a) are the analysis domains, which represent three typical irrigated areas over the Yellow River basin, based on the MODIS potential irrigation area fraction. The land cover/land use abbreviations in (b) are as follows: ENF, evergreen needleleaf forest; EBF, evergreen broadleaf forest; DNF, deciduous needleleaf forest; DBF, deciduous broadleaf forest; MF, mixed forest; CSH, closed shrubland; OSH, open shrubland; WSA, woody savanna; SAV, savanna; GRA, grassland; WET, permanent wetland; CRO, cropland; URB, urban and built-up land; CNV, cropland/natural vegetation mosaic; SNO, snow and ice; BAR, barren; WAT, water body; OTH, other.

$$MA = \frac{SM - SM_{wp}}{SM_{fc} - SM_{wp}}, \quad (2)$$

where SM is the current root-zone soil moisture, and  $SM_{wp}$  and  $SM_{fc}$  are the soil wilting point and field capacity, respectively.

### 3. Results

#### 3.1. Model evaluation

In this study, the performance of the CTL run was evaluated in terms of  $T_{2m}$  (mean surface air temperature at 2 m) and precipitation by comparing the simulated results with observations (denoted as OBS) obtained from observation stations over the Yellow River basin. The results indicated that the CTL run captured the observed  $T_{2m}$  and precipitation reasonably well. Figure 2(a)–(c) show the spatial patterns of the long-term summer mean (2001–2010)  $T_{2m}$  derived from OBS, CTL, and IRR output. All results (CTL, IRR, and OBS) showed the  $T_{2m}$  as having the same spatial pattern. The CTL and IRR simulations were slightly colder than OBS in the west of the Yellow River basin, as most of this area is located in the plateau region, where the number of meteorological stations is far fewer and the bias is thus greater. However, in most parts of the Yellow River basin, especially the middle and lower reaches of the Yellow River, the simulated temperature was slightly warmer than OBS. Figure 2(e)–(g) show the spatial patterns of OBS, CTL, and IRR precipitation over the model domain. The precipitation field from the CTL and IRR simulations captured the main pattern of OBS precipitation, although both the magnitudes of CTL and IRR were overestimated in the southeast of the Yellow River basin.

#### 3.2. Simulated irrigation effects

Figure 2(d) shows that the JJA (June–August) mean  $T_{2m}$  for IRR decreased by 0.1–0.4 K for areas where irrigation occurs. The mean reductions in  $T_{2m}$  due to irrigation were 0.1 K within both region 2 and region 3, while there was little change in region 1 (Table 1). Figure 2(h) shows the precipitation change was not consistent with the  $T_{2m}$ . The difference occurred not only over the irrigated regions, but also in surrounding irrigated regions. The precipitation change between IRR and CTL decreased over the irrigated regions but increased in surrounding irrigated regions; as

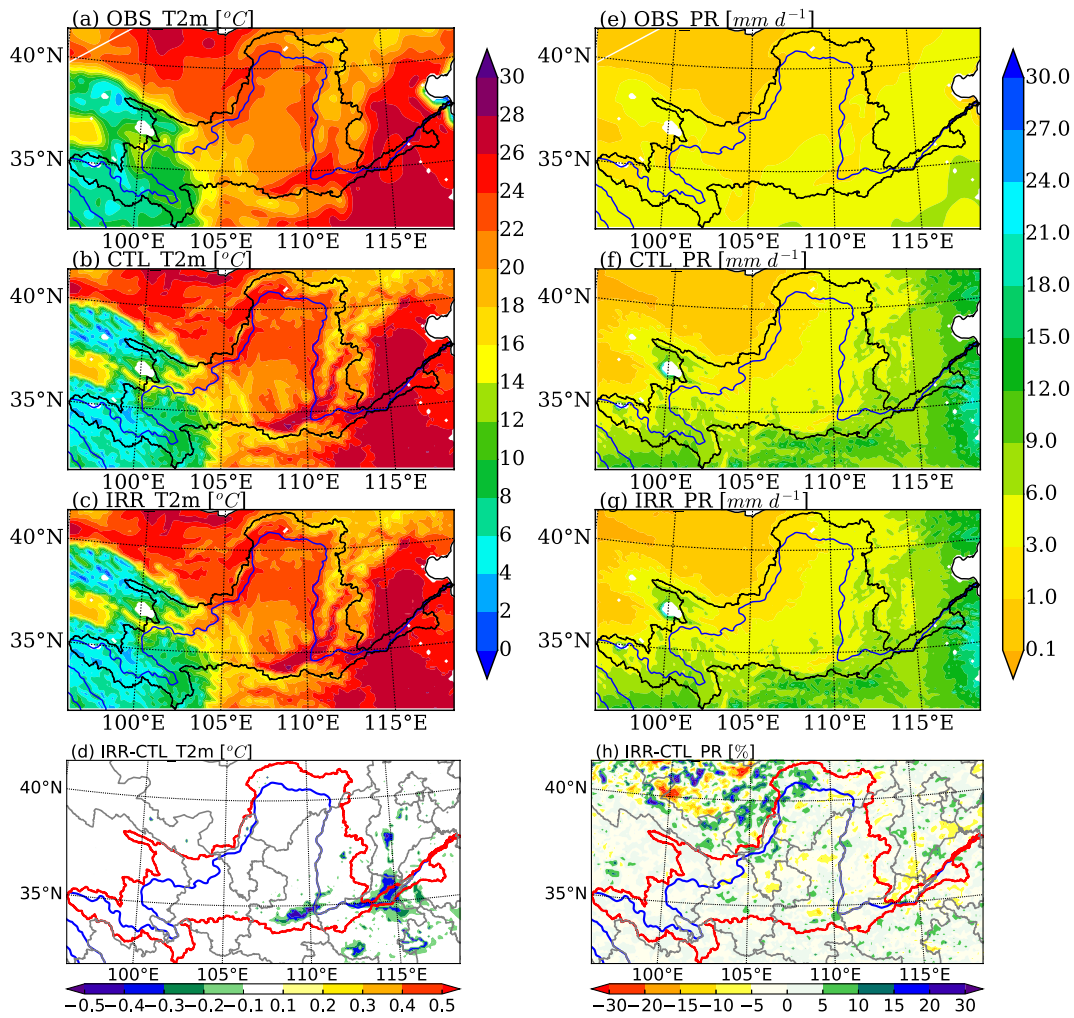


**Figure 2.** Observed (OBS) and simulated (IRR and CTL) three-month (June–August) mean  $T_{2m}$  (mean surface air temperature at 2 m; units:  $^{\circ}\text{C}$ ) and precipitation (units:  $\text{mm d}^{-1}$ ) during 2001–2010, and their differences between the simulation with irrigation (IRR) and the control run (CTL): (a)  $T_{2m}$  in OBS; (b)  $T_{2m}$  in CTL; (c)  $T_{2m}$  in IRR; (d)  $T_{2m}$  difference between IRR and CTL; (e) PR in OBS; (f) PR in CTL; (g) PR in IRR; (h) PR difference between IRR and CTL.

Qian et al. (2013) indicated, we cannot investigate possible precipitation effects downstream within a limited model domain. When irrigation occurs, the land surface receives additional water and the soil moisture increases due to irrigation (not shown) after each irrigation event, ultimately leading to increased evapotranspiration and thus increased LH flux. The increase in LH flux (evapotranspiration) will in turn lead to increased movement of water vapor from the land surface into the atmosphere, thus causing more cloud cover. This will then result in increased reflection of shortwave radiation and a decrease in total downward radiation, and this change in radiation will strengthen the cooling effect. In the present study, this decreased temperature resulted in a corresponding decrease in upwelling longwave radiation over the three irrigated regions, and caused the net radiation to change.

In all, the net radiation increased by  $0.1 \text{ W m}^{-2}$  in region 1, by  $1.1 \text{ W m}^{-2}$  in region 2, and by  $0.8 \text{ W m}^{-2}$  in region 3 (Table 1). Figure 3 shows the spatial patterns and their differences in sensible heat (SH) and LH for JJA between IRR and CTL. The simulation results showed a decrease in summer mean SH and an increase in summer mean LH. The SH decreased by  $1.0 \text{ W m}^{-2}$  in region 1, by  $3.2 \text{ W m}^{-2}$  in region 2, and by  $2.0 \text{ W m}^{-2}$  in region 3; while the LH increased by  $1.1 \text{ W m}^{-2}$  in region 1, by  $3.8 \text{ W m}^{-2}$  in region 2, and by  $2.3 \text{ W m}^{-2}$  in region 3 (Table 1). The largest increase in summer mean LH occurred in the lower reaches of the Yellow River basin, where the irrigation area fraction was large in IRR. The surface energy budgets appear to have changed little for non-irrigated areas. Irrigation increased the LH fluxes and decreased the SH fluxes, thereby leading to a direct evaporative cooling of the surface.

**Table 1.** Differences (IRR minus CTL) of temperature and fluxes for the three regions shown in Figure 1.

Region	Run	$T_{2m}$ (°C)	SH ( $\text{W m}^{-2}$ )	LH ( $\text{W m}^{-2}$ )	G ( $\text{W m}^{-2}$ )	LWU ( $\text{W m}^{-2}$ )	LWD ( $\text{W m}^{-2}$ )	SWU ( $\text{W m}^{-2}$ )	SWD ( $\text{W m}^{-2}$ )	RN ( $\text{W m}^{-2}$ )
1	IRR	24.2	74.7	40.0	-4.1	434.7	338.2	80.5	316.2	139.2
	CTL	24.2	75.7	38.9	-4.0	435.2	338.2	80.6	316.7	139.1
	Diff	0.0	-1.0	1.1	-0.1	-0.5	0.0	-0.1	-0.5	0.1
2	IRR	23.9	50.1	97.7	-3.1	433.3	363.9	52.2	285.3	163.7
	CTL	24.0	53.3	93.9	-2.6	435.0	364.5	52.2	285.2	162.6
	Diff	-0.1	-3.2	3.8	-0.5	-1.7	-0.6	0.0	0.1	1.1
3	IRR	26.1	48.7	98.6	-3.1	443.9	379.7	56.3	288.0	167.5
	CTL	26.2	50.7	96.3	-2.6	445.0	380.2	56.3	287.9	166.7
	Diff	-0.1	-2.0	2.3	-0.5	-1.1	-0.5	0.0	0.1	0.8

Notes: IRR, simulation with irrigation; CTL, control run;  $T_{2m}$ , 2 m surface air temperature; SH, sensible heat flux; LH, latent heat flux; G, soil heat flux; LWU, upwelling longwave flux; LWD, downwelling longwave flux; SWU, upwelling shortwave flux; SWD, downwelling shortwave flux; RN, net radiation flux; Diff, difference.

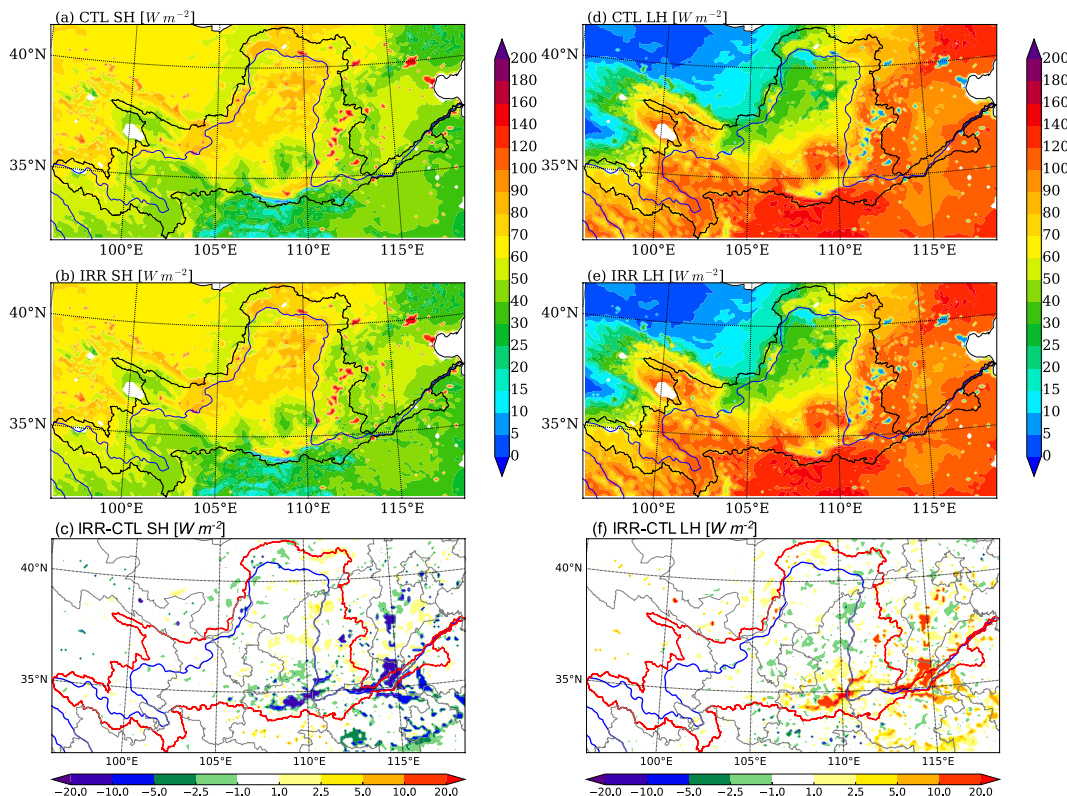


**Figure 3.** Three-month (June–August) mean SH (sensible heat flux; units:  $\text{W m}^{-2}$ ) and LH (latent heat flux; units:  $\text{W m}^{-2}$ ) during 2001–2010, and their differences between the simulation with irrigation (IRR) and the control run (CTL): (a) SH in CTL; (b) SH in IRR; (c) SH difference between IRR and CTL; (d) LH in CTL; (e) LH in IRR; (f) LH difference between IRR and CTL.

Qian et al. (2013) indicated that change in the planetary boundary layer height (PBLH) is very important in cloud and land surface feedbacks, and the lifting condensation level (LCL) is affected by the distribution of surface fluxes. Figure 4(a) and (b) show that both the PBLH and LCL decreased over irrigated regions, especially in region 3, home to the largest levels of irrigation. Figure 4(c) shows the difference values between  $|d\text{LCL}|$  and  $|d\text{PBLH}|$  were positive (the LCL was less than the

PBLH) over most irrigated areas, meaning the formation of shallow cloud was more likely. An increase in the water vapor inputs from land to atmosphere will increase the humidity in the lower PBL, which may lead to a decrease in the LCL. Meanwhile, an increase in the amount of shallow cloud formation may reduce shortwave radiation reaching surface, which might then impact the partitioning of surface fluxes and soil moisture, and ultimately the  $T_{2m}$  and precipitation distribution.

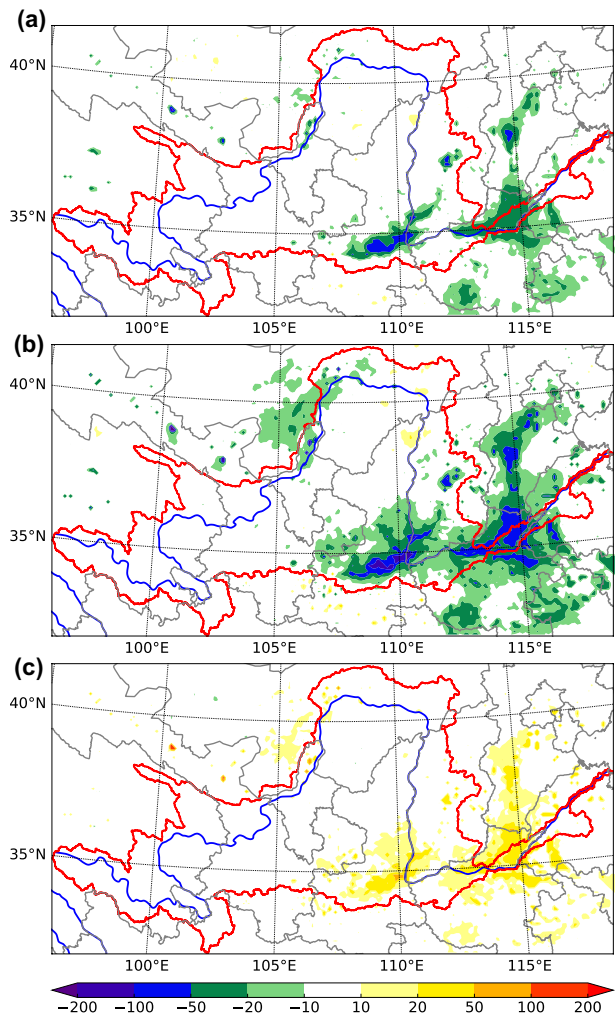


**Figure 4.** (a) Average difference in the simulated planetary boundary layer height (PBLH; units: m) between the simulation with irrigation (IRR) and the control run (CTL) (i.e. IRR minus CTL;  $|dPBLH|$ ) during 2001–2010. (b) As in (a), but for the lifting condensation level (LCL; units: m;  $|dLCL|$ ). (c) As in (a), but for  $|dLCL|$  minus  $|dPBLH|$  (units: m).

#### 4. Discussion and conclusions

In this study, we investigated the impacts of agricultural irrigation on the  $T_{2m}$  and surface heat fluxes over the Yellow River basin. Based on the modeling results, we examined the changes in  $T_{2m}$  and heat fluxes between IRR and CTL. The results indicated that the surface air temperature at 2 m and energy budgets were very sensitive to the presence of irrigation over the Yellow River basin. Including the irrigation scheme in the regional climate model led to a decrease in  $T_{2m}$  over irrigated areas. Irrigation adds more water to the land surface and leads to an increase in soil moisture. Thus, evapotranspiration and LH increase at the land surface. The model results showed that the agricultural irrigation caused LH flux increases, while the SH flux decreased. The cooling effect was consistent with the changes in evapotranspiration and heat fluxes due to

irrigation over the Yellow River basin. It was also found that agricultural irrigation decreased the PBLH and LCL; but, the decrease in the LCL was greater than the decrease in the PBLH, meaning an increase in cloud formation was more likely, leading to changes in soil moisture and the spatial distribution of surface fluxes, which ultimately affected the  $T_{2m}$  and precipitation.

In the future, we intend to extend this work by using different irrigation methods to assess the impact of irrigation on regional climate and hydrological cycles. We will also evaluate the impact of model resolution and model physics on the simulations.

#### Disclosure statement

No potential conflict of interest was reported by the authors.

#### Funding

The work was supported by the National Key Research and Development Program of China [grant number 2016YFA0600403], the National Natural Science Foundation of China [grant numbers 41305062, 41530532]; the China Special Fund for Meteorological Research in the Public Interest [grant number GYHY201506001-1].

#### References

- Adegoke, J. O., R. A. Pielke Sr, J. Eastman, R. Mahmood, and K. G. Hubbard. 2003. "Impact of Irrigation on Midsummer Surface Fluxes and Temperature under Dry Synoptic Conditions: A Regional Atmospheric Model Study of the U.S. High Plains." *Monthly Weather Review* 131 (3): 556–564.
- Adegoke, J. O., R. A. Pielke Sr, and A. M. Carleton. 2007. "Observational and Modeling Studies of the Impacts of Agriculture-related Land Use Change on Planetary Boundary Layer Processes in the Central US." *Agricultural and Forest Meteorology* 142: 203–215.
- Barnston, A. G., and P. T. Schickedanz. 1984. "The Effect of Irrigation on Warm Season Precipitation in the Southern Great Plains." *Journal of Climate and Applied Meteorology* 23 (6): 865–888.
- Chen, L., Y. Li, F. Chen, A. Barr, M. Barlage, and B. Wan. 2016. "The Incorporation of an Organic Soil Layer in the Noah-MP Land Surface Model and Its Evaluation over a Boreal Aspen Forest." *Atmospheric Chemistry and Physics* 16: 8375–8387. doi: 10.5194/acp-16-8375-2016.
- Dee, D. P., S. M. Uppala, A. J. Simmons, P. Berrisford, P. Poli, S. Kobayashi, U. Andrae, et al. 2011. "The ERA-Interim Reanalysis: Configuration and Performance of the Data Assimilation System." *Quarterly Journal of the Royal Meteorological Society* 137: 553–597. doi: 10.1002/qj.828.
- Diffenbaugh, N. S. 2009. "Influence of Modern Land Cover on the Climate of the United States." *Climate Dynamics* 33 (7–8): 945–958.
- Douglas, E. M., A. Beltrán-Przekurat, D. Niyogi, R. A. Pielke Sr, C. J. Vörösmarty, et al. 2009. "The Impact of Agricultural Intensification and Irrigation on Land–Atmosphere Interactions



- and Indian Monsoon Precipitation – A Mesoscale Modeling Perspective." *Global and Planetary Change* 67 (1–2): 117–128.
- Kueppers, L. M., M. A. Snyder, and L. C. Sloan. 2007. "Irrigation Cooling Effect: Regional Climate Forcing by Land-use Change." *Geophysical Research Letters* 34 (3): L03703.
- Lee, E., T. N. Chase, B. Rajagopalan, R. G. Barry, T. W. Biggs, and P. J. Lawrence. 2009. "Effects of Irrigation and Vegetation Activity on Early Indian Summer Monsoon Variability." *International Journal of Climatology* 29 (4): 573–581.
- Lei, M., Z. Jia, and S. Xiao. 2013. "Study of Agricultural Development Scale of the Yellow River Basin." *Yellow River* 35 (10): 99–103.
- Leng, G., M. Huang, Q. Tang, H. Gao, and L. R. Leung. 2014. "Modeling the Effects of Groundwater-fed Irrigation on Terrestrial Hydrology over the Conterminous United States." *Journal of Hydrometeorology* 15 (3): 957–972.
- Lobell, D. B., and C. Bonfils. 2008. "The Effect of Irrigation on Regional Temperatures: A Spatial and Temporal Analysis of Trends in California, 1934–2002." *Journal of Climate* 21 (10): 2063–2071.
- Ma, Z. G., H. L. Wei, and C. B. Fu. 1999. "Progress in the Research on the Relationship between Soil Moisture and Climate Change." *Advance in Earth Sciences* 14 (3): 300–305. (in Chinese).
- Moore, N., and S. Rojstaczer. 2001. "Irrigation-induced Rainfall and the Great Plains." *Journal of Applied Meteorology* 40 (8): 1297–1309.
- Ozdogan, M., and G. Gutman. 2008. "A New Methodology to Map Irrigated Areas Using Multi-temporal MODIS and Ancillary Data: An Application Example in the Continental US." *Remote Sensing of Environment* 112 (9): 3520–3537.
- Ozdogan, M., M. Rodell, H. K. Beaudoin, and D. L. Toll. 2010. "Simulating the Effects of Irrigation over the United States in a Land Surface Model Based on Satellite-Derived Agricultural Data." *Journal of Hydrometeorology* 11 (1): 171–184.
- Pielke, R. A., J. Adegoke, A. Beltran-Przekurat, C. A. Hiemstra, J. Lin, U. S. Nair, D. Niyogi, et al. 2007. "An Overview of Regional Landuse and Land-Cover Impacts on Rainfall." *Tellus Series B-Chemical and Physical Meteorology* 59 (3): 587–601.
- Qian, Y., M. Huang, B. Yang, and L. K. Berg. 2013. "A Modeling Study of Irrigation Effects on Surface Fluxes and Land-Air-Cloud Interactions in the Southern Great Plains." *Journal of Hydrometeorology* 14 (3): 700–721. doi:[10.1175/JHM-D-12-0134.1](https://doi.org/10.1175/JHM-D-12-0134.1).
- Sacks, W. J., B. I. Cook, N. Buennning, S. Levis, and J. H. Helkowski. 2009. "Effects of Global Irrigation on the near-Surface Climate." *Climate Dynamics* 33 (2–3): 159–175.
- Shiklomanov, I. A. 2000. "Appraisal and Assessment of World Water Resources." *Water International* 25: 11–32.
- Siebert, S., P. Doll, S. Feick, and J. Hoogeveen. 2005. *Global Map of Irrigated Areas Version 3.0*. Frankfurt am Main, Germany/FAO, Rome, Italy: Johann Wolfgang Goethe University.
- Tang, Q., T. Oki, S. Kanae, and H. Hu. 2007. "The Influence of Precipitation Variability and Partial Irrigation within Grid Cells on a Hydrological Simulation." *Journal of Hydrometeorology* 8: 499–512. doi:[10.1175/JHM589.1](https://doi.org/10.1175/JHM589.1).
- Yu, T., D. W. He, and J. S. Chen. 2003. "Impact of Quantity of River Water by Irrigation in a Yellow River Basin." *Journal of Agro-Environment Science* 22 (6): 664–668. (in Chinese).